



Sub-monolayer quantum dots in confinement enhanced dots-in-a-well heterostructure

S. Sengupta, J. O. Kim, A. V. Barve, S. Adhikary, Y. D. Sharma, N. Gautam, S. J. Lee, S. K. Noh, S. Chakrabarti, and S. Krishna

Citation: [Applied Physics Letters](#) **100**, 191111 (2012); doi: 10.1063/1.4711214

View online: <http://dx.doi.org/10.1063/1.4711214>

View Table of Contents: <http://scitation.aip.org/content/aip/journal/apl/100/19?ver=pdfcov>

Published by the [AIP Publishing](#)

Articles you may be interested in

[Multi-stack InAs/InGaAs sub-monolayer quantum dots infrared photodetectors](#)

Appl. Phys. Lett. **102**, 011131 (2013); 10.1063/1.4774383

[Bias mediated tuning of the detection wavelength in asymmetrical quantum dots-in-a-well infrared photodetectors](#)

Appl. Phys. Lett. **93**, 203512 (2008); 10.1063/1.3033169

[High quantum efficiency dots-in-a-well quantum dot infrared photodetectors with AlGaAs confinement enhancing layer](#)

Appl. Phys. Lett. **92**, 193506 (2008); 10.1063/1.2926663

[Influence of quantum well and barrier composition on the spectral behavior of InGaAs quantum dots-in-a-well infrared photodetectors](#)

Appl. Phys. Lett. **91**, 173508 (2007); 10.1063/1.2802559

[Origin of photocurrent in lateral quantum dots-in-a-well infrared photodetectors](#)

Appl. Phys. Lett. **88**, 213510 (2006); 10.1063/1.2207493

An advertisement for COMSOL Multiphysics simulation projects. The background is dark with a grid pattern. On the left, there is a 3D cutaway illustration of a cylindrical component with a red interior and a blue exterior, showing a light beam passing through it. The text 'Over 600 Multiphysics Simulation Projects' is prominently displayed in white and blue. A blue button with white text says 'VIEW NOW >>'. The COMSOL logo is in the bottom right corner.

Sub-monolayer quantum dots in confinement enhanced dots-in-a-well heterostructure

S. Sengupta,¹ J. O. Kim,² A. V. Barve,² S. Adhikary,¹ Y. D. Sharma,² N. Gautam,² S. J. Lee,³ S. K. Noh,³ S. Chakrabarti,¹ and S. Krishna^{2,a)}

¹Centre for Nanoelectronics, Department of Electrical Engineering, Indian Institute of Technology Bombay, Mumbai-400076, India

²Center for High Technology Materials, Department of Electrical and Computer Engineering, University of New Mexico, Albuquerque, New Mexico 87106, USA

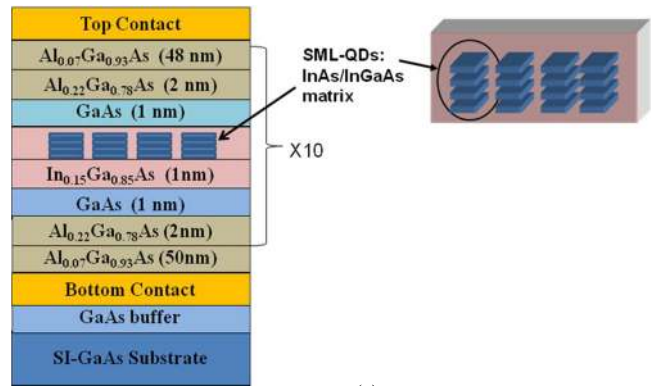
³Korean Research Institute of Standards and Science, Daejeon 305340, South Korea

(Received 2 March 2012; accepted 17 April 2012; published online 9 May 2012)

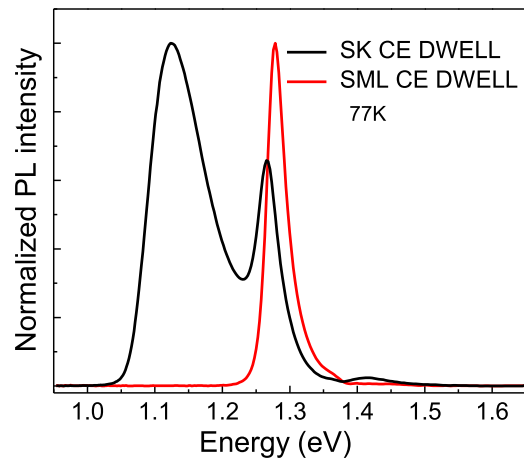
We have investigated optical properties and device performance of sub-monolayer quantum dots infrared photodetector with confinement enhancing (CE) barrier and compared with conventional Stranski-Krastanov quantum dots with a similar design. This quantum dots-in-a-well structure with CE barrier enables higher quantum confinement and increased absorption efficiency due to stronger overlap of wavefunctions between the ground state and the excited state. Normal incidence photoresponse peak is obtained at $7.5\ \mu\text{m}$ with a detectivity of $1.2 \times 10^{11}\ \text{cm Hz}^{1/2}\ \text{W}^{-1}$ and responsivity of $0.5\ \text{A/W}$ (77 K, 0.4 V, $f/2$ optics). Using photoluminescence and spectral response measurements, the bandstructure of the samples were deduced semi-empirically. © 2012 American Institute of Physics. [<http://dx.doi.org/10.1063/1.4711214>]

In the recent past, quantum dots (QD) infrared photodetectors (QDIP) based on Stranski-Krastanov (SK) QD have been extensively researched due to the advantages of the three dimensional confinement of carriers which provide intrinsic sensitivity to normal incidence radiation,¹ lower dark current,² and long excited state lifetime.³ Several groups have contributed to the drastic improvement of QDIP by introducing different material compositions and novel architectures like quantum dots in-a-well (DWELL),^{4,5} quantum dots in double well (DDWELL),^{6,7} and successfully demonstrated high performance devices.^{8–10} A typical DWELL structure, where InAs quantum dots are confined inside a InGaAs-GaAs quantum well (QW) offers the advantage of tuning the detection peak wavelength,¹¹ while providing lower dark current⁷ and higher operating temperature.¹² In order to increase the absorption quantum efficiency (QE) and confinement of electron wave-function, confinement enhancing (CE) barriers surrounding the dots have been introduced recently.¹³ Barve *et al.* suggest a different architecture, where a 2 nm thick $\text{Al}_{0.22}\text{Ga}_{0.78}\text{As}$ CE barriers are employed around the entire DWELL structure.¹⁴ Presence of such blocking layers in the transport direction reduces the dark current significantly while providing the advantages of enhanced absorption coefficient and high escape probability.

While a considerable effort has been made to improve the barrier design, very few studies have been done beyond the idea of SK QD. Due to the nature of formation, SK dots always have an InAs wetting layer, which actually reduces the degree of confinement of carriers and does not contribute to the normal incidence absorption. Sub-monolayer (SML) QD based design has emerged as a promising solution of this problem.^{15–18} SML QD structure is typically grown by depositing fraction of a monolayer of InAs in a GaAs or



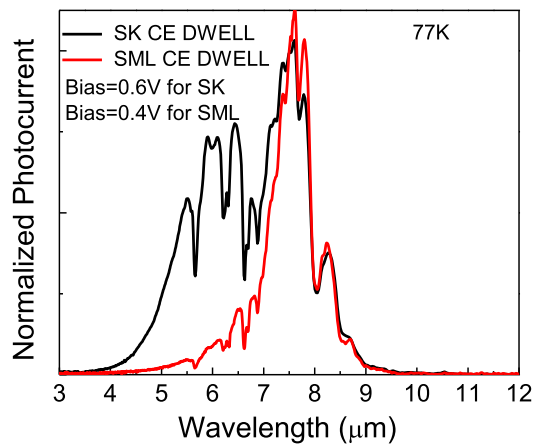
(a)



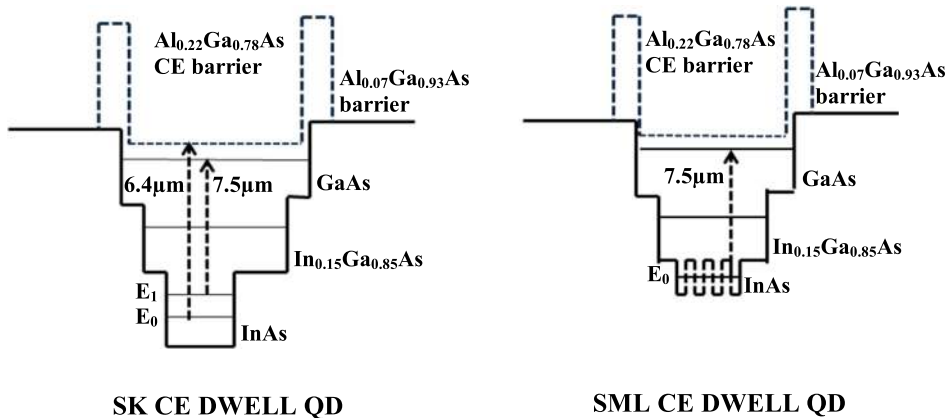
(b)

FIG. 1. (a) Schematic of SML CE DWELL heterostructure. Four stacks of InAs are deposited in InGaAs matrix. InAs/InGaAs structure is embedded in GaAs quantum well and surrounded by $\text{Al}_{0.22}\text{Ga}_{0.78}\text{As}$ CE barrier. (b) Comparison of normalized PL spectra of SML CE DWELL QD and SK CE DWELL QD. The ground state of SML QD shifts towards shorter wavelength compared to SK QD due to reduced size of dots. Note that the ground state of SML QD coincides with 1st excited state of SK QD.

^{a)}Author to whom correspondence should be addressed. Electronic mail: skrishna@chtm.unm.edu.



(a)



(b)

FIG. 2. (a) Spectral response comparison between SML CE DWELL QD and SK CE DWELL QD at 77 K. Photocurrent response from the SK QD contains two main peaks at 6.4 μm and 7.5 μm , the SML QD sample shows response at 7.5 μm . (b) The bandstructures of SML CE DWELL QD and SK CE DWELL QD samples, constructed on the basis of PL and spectral response measurements. The origin spectral response peaks for SK QD is transition between ground state and excited state of the QD and the excited state in the QW. The spectral response for SML QD obtained due to the transition between ground state of the QD to the excited state in the QW.

InGaAs QW. In this way, the formation of any wetting layer is avoided which causes better quantum confinement and increased carrier wave-function overlap. Moreover, such SML QD offers higher density of dots due to smaller (~ 5 nm) lateral size and narrow average lateral spacing (~ 2 nm) between two dots which leads to a higher absorption efficiency.^{19,20} Several reports of SML QD based lasers can be found in the literature, but there are only a few reports on a SML QD infrared photodetector.^{16,19} The typical operating bias for SML QD detector, which is less than 1 V, is suitable for focal plane array (FPA) applications. Performance of SML QD based device can be further improved by planting the dots into a CE DWELL structure to reduce the operating bias while maintaining good absorption quantum efficiency. In this paper, we report on a SML QD in a confinement enhanced DWELL structure operating at 77 K with a detection peak wavelength of 7.5 μm with a high detectivity of 1.2×10^{11} cm Hz^{1/2} W⁻¹ at only 0.4 V operating bias. Absorption quantum efficiency is measured to be 7.0% at the same applied bias. We have also compared the performance of the above mentioned device with a device based on SK QD with the similar heterostructure.

The sample under consideration is grown by molecular beam epitaxy (MBE) equipped with As₂ cracker source on a semi-insulating GaAs (0 0 1) substrate. We have performed a systematic study on InAs SML, including optimization of different growth parameters like the flux ratio, growth tem-

perature, thickness of InAs deposition, and variations using different material compositions. The active region of the sample, as shown in Fig. 1(a), consists of four vertically stacked 0.3ML InAs layers inside a 4.3 nm thick In_{0.15}Ga_{0.85}As QW, surrounded by 1 nm GaAs QW—2 nm Al_{0.22}Ga_{0.78}As CE barrier—48 nm Al_{0.07}Ga_{0.93}As barrier. This stack is repeated 10 times. Initially, the 50 nm Al_{0.07}Ga_{0.93}As barrier and CE barrier were grown and capped with 1 nm GaAs layer at 590 °C. Then the substrate temperature was reduced to 500 °C to grow InGaAs QW with Si doped InAs SML QD with 10 s interruption time before and after each InGaAs and InAs deposition. Then, the structure was covered with 1 nm GaAs layer and the temperature was raised to 590 °C with interruption of 180 s. The CE barrier is designed such that the excited energy level in the QW is close to the continuum energy level, which provides high absorption efficiency, high escape probability, and low bias operation. We have chosen another sample with same design with conventional SK QD instead of SML dots to compare the optical property and device performance.¹⁴

To obtain information about the bandstructure of our samples, we have performed room temperature photoluminescence (PL) measurements. The experiment was done using Ar⁺⁺ laser with power of 2 W and InGaAs detector. Fig. 1(b) depicts normalized PL spectra obtained from the SML QD and SK QD samples. For SK QD, the ground state emission peak is at 1.12 eV while the ground state emission

peak for SML QD is observed at 1.28 eV. The observed blue shift in the ground state PL peak is possibly due to lesser Indium in the SML QD ($\sim 1.2\text{ML}$) compared to the SK QDs (2-2.4ML). The narrower full-width-half-maximum (FWHM) of PL spectrum of SML QD suggests high uniformity of the QD size distribution. Fluence dependent PL experiment confirms the existence of the 1st excited state in SK QD which appears at 1.27 eV. It should be noted that the ground state energy level of SML QD is close to the energy level of 1st excited state of SK QD.

Devices were processed into $410 \times 410 \mu\text{m}^2$ square detectors using a standard method of optical lithography, plasma etching, and contact metallization. A liquid nitrogen cooled cryostat and Nicolet 550 Fourier transform infrared spectrometer were used to measure the spectral response at 77 K. Fig. 2(a) depicts the comparison of spectral response from SK dots and SML dots in the CE DWELL architecture. While the photocurrent response from the SK QD shows two main peaks at $6.5 \mu\text{m}$ and $7.5 \mu\text{m}$, the SML QD sample shows response at $7.5 \mu\text{m}$ only. The detailed analysis of SK dots in CE DWELL is reported elsewhere.¹⁴ The photocurrent peak of SML QD shows a symmetric behavior for the both polarities of applied bias voltage. The peak at $7.5 \mu\text{m}$ for SK QD is identified as the transition between the excited state of the QD (E_1) to the excited state in the QW. The origin of $7.5 \mu\text{m}$ in SML QD is due to the transition between the ground state of the QD (E_0) to the excited state in the QW. Appearance of photocurrent response peak at $7.5 \mu\text{m}$ for both samples supports our conclusions from PL measurement. Combining the information from PL experiment and spectral response measurement, we have semi-empirically reconstructed the bandstructures of heterostructures which are shown in Fig. 2(b).

Radiometric measurements were carried out by using a blackbody source calibrated at 900 K to measure detectivity (D^*) and responsivity (R) of the devices at 77 K. The D^* and R are calculated using the following equations:

$$D^* = R(\Delta f)^{1/2}/i_n \text{ and } R = e g \eta / (h\nu), \quad (1)$$

where A is area of the detector, Δf is band-width, i_n is noise current, e is electronic charge, g is photoconductive (PC) gain, η is absorption quantum efficiency, and $h\nu$ is photoexcitation energy. By comparing the measured photocurrent with the dark current, both the devices were found to be background limited infrared photodetector (BLIP) at 77 K. In Fig. 3(a), results of D^* measurement are shown. The highest D^* for SML QD is found to be $1.2 \times 10^{11} \text{ cm Hz}^{1/2} \text{ W}^{-1}$ at 0.4 V bias voltage, which is higher than previously reported results for SML QD although at a lower operating bias.¹⁶ The recorded D^* for SML QD is found as a factor of two higher than the SK QD device. Fig. 3(b) compares the responsivity of two devices, which shows a significant improvement of R over the whole bias range. As the detection peak is due to the transition between bound state in QD and excited energy in the QW, which is close to the continuum energy level, the escape probability of photocarriers is higher. This results low value of operational bias and high responsivity. High responsivity also indicates high value of absorption QE. The noteworthy low operating bias voltage

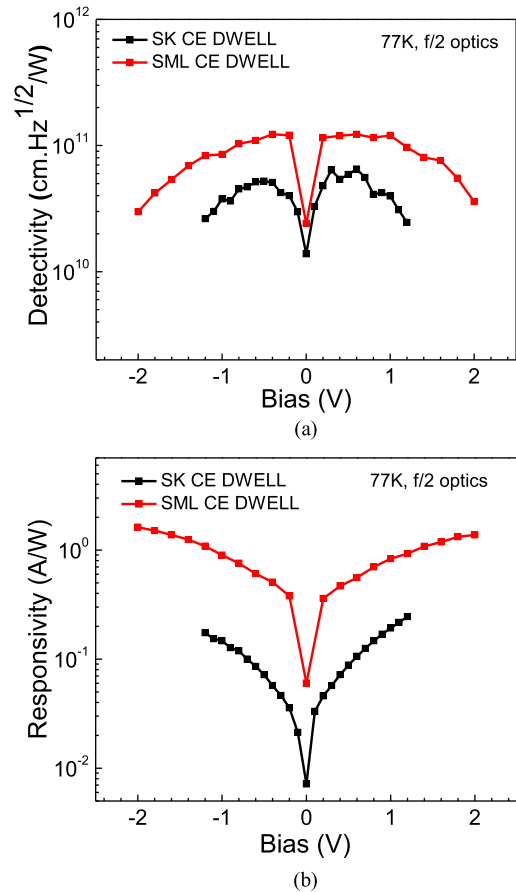


FIG. 3. (a) Comparison of detectivity measurements between SML CE DWELL QD and SK CE DWELL QD (77 K, $f/2$ optics), showing an improvement in D^* value for SML CE DWELL QD device. (b) Responsivity measurements of SML CE DWELL QD and SK CE DWELL QD samples (77 K, $f/2$ optics). Responsivity of SML QD is found to be more than 4 times higher than that of SK QD at a same bias.

indicates its feasibility for fabrication of FPA using commercially available silicon read-out circuits.

To understand the transport mechanism inside the SML QD device we measured the photoconductive gain to estimate absorption QE of SML QD device. The device was irradiated by a blackbody source at 900 K during the measurement of the PC gain to ensure the device was photon noise limited. The PC gain is calculated using the following equation

$$G_{\text{ph}} = i_{\text{ph}}^2 / (4e \Delta f I_{\text{ph}}), \quad (2)$$

where i_n , e , Δf , and I_{ph} are noise current, electronic charge, noise band-width, and photocurrent, respectively. Fig. 4(a) shows the results of PC gain and absorption quantum efficiency at 77 K. The PC gain is found to be lower than unity at operating bias region. Due to probable existence of excited states in QW, the capture probability is high which justifies such low value of PC gain. The absorption efficiency reaches to around 7.0% at the operating bias and increases up to 11.5% as bias is increased further. Such high value of absorption QE is attributed to strong overlap of electronic wavefunction inside the dots. In addition to the presence of AlGaAs layer, the smaller size of the dots is responsible for the better wavefunction coupling which enhances the

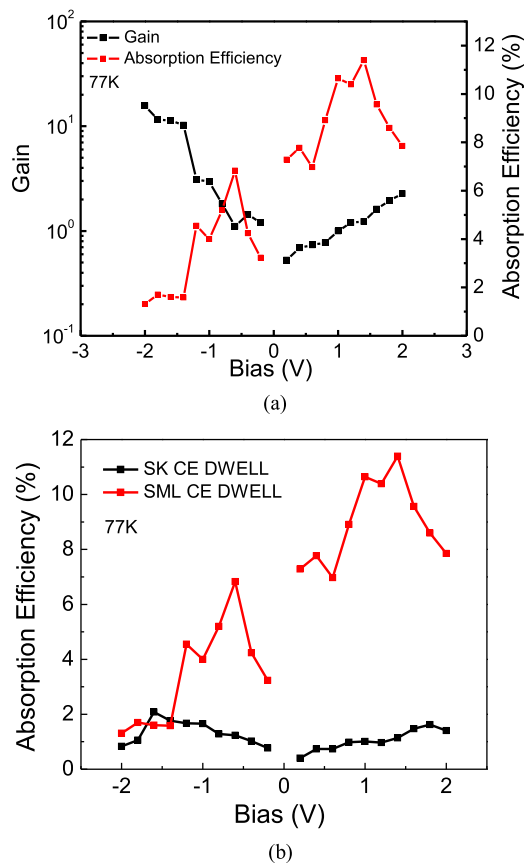


FIG. 4. (a) Results of photoconductive gain and absorption efficiency measurement of SML CE DWELL is shown. Such high value of absorption efficiency is attributed to strong coupling of wavefunctions of the carriers. (b) Comparison of absorption efficiency measurement of SML CE DWELL QD and SK CE DWELL QD. A notable enhancement is found in absorption efficiency for SML CE DWELL.

absorption strength of ground state electrons. Fig. 4(b) clearly indicates a considerable enhancement in absorption QE for SML CE DWELL compared to its SK counterpart. High values of detectivity, PC gain, and absorption QE are obtained even at zero bias. This is due to the limitation of measurement setup during noise measurement and hence those results are ignored.

In conclusion, infrared photodetector based on SML QD has been presented and compared with traditional SK QD in CE DWELL architecture. Our design of SML QD exhibits better performance compared to previously recorded citations. We have also investigated the optical properties of SML QD to understand the structure of different energy levels. The device characterization results ensure high perform-

ance at low operating bias at 77 K. Higher confinement and better overlap of wavefunctions between the ground state of the quantum dot and excited state of the quantum well are achieved owing to the presence of CE barrier and smaller size of dots. Detectivity of the SML based device is measured as $1.2 \times 10^{11} \text{ cm Hz}^{1/2} \text{ W}^{-1}$ with responsivity reaching up to 0.5 A/W (77 K, 0.4 V, 7.5 μm , $f/2$ optics).

This work is supported by AFOSR FA9550-09-1-0410, AFRL FA9453-12-1-0336, PST-2010-136, and KRIS-GRL Program. Partial funding from Department of Science and Technology, India is acknowledged.

- ¹D. Pan, E. Towe, and S. Kennerly, *Appl. Phys. Lett.* **73**, 1937 (2003).
- ²A. Stiff, S. Krishna, P. Bhattacharya, and S. Kennerly, *Appl. Phys. Lett.* **79**, 421 (2001).
- ³U. Bockelmann and G. Bastard, *Phys. Rev. B* **42**, 8947 (1990).
- ⁴S. Krishna, *J. Phys. D: Appl. Phys.* **38**, 2142 (2005).
- ⁵L. Höglund, C. Asplund, Q. Wang, S. Almqvist, H. Malm, E. Petrini, J. Y. Andersson, P. O. Holtz, and H. Pettersson, *Appl. Phys. Lett.* **88**, 213510 (2006).
- ⁶Y. D. Sharma, M. N. Kutty, R. V. Shenoi, A. V. Barve, S. Myers, J. Shao, E. Plis, S. Lee, S. Noh, and S. Krishna, *J. Vac. Sci. Technol. B* **28**, C3G1 (2010).
- ⁷X. Han, J. Li, J. Wu, G. Cong, X. Liu, Q. Zhu, and Z. Wang, *J. Appl. Phys.* **98**, 053703 (2005).
- ⁸S. D. Gunapala, S. V. Bandara, C. J. Hill, D. Z. Ting, J.K. Liu, B. Rafol, E. R. Blazejewski, J. M. Mumolo, S. A. Keo, S. Krishna, Y.C. Chang, and C. A. Shott, *IEEE J. Quantum Electron.* **43**, 230 (2007).
- ⁹S. Chakrabarti, A. D. Stiff-Roberts, X. H. Su, P. Bhattacharya, G. Ariyawansa, and A.G. U. Perera, *J. Phys. D: Appl. Phys.* **38**, 2135 (2005).
- ¹⁰L. Fu, P. Lever, K. Sears, H. H. Tan, and C. Jagadish, *IEEE Electron Device Lett.* **26**, 628 (2005).
- ¹¹G. Ariyawansa, A. Perera, G. Raghavan, G. von Winckel, A. Stintz, and S. Krishna, *IEEE Photon. Technol. Lett.* **17**, 1064 (2005).
- ¹²A. V. Barve, J. Montaya, Y. Sharma, T. Rotter, J. Shao, W.-Y. Jang, S. Meesala, S. J. Lee, and S. Krishna, *Infrared Phys. Technol.* **54**, 215 (2011).
- ¹³H. S. Ling, S. Y. Wang, C. P. Lee, and M. C. Lo, *Appl. Phys. Lett.* **92**, 193506 (2008).
- ¹⁴A. V. Barve, S. Sengupta, J. O. Kim, Y. D. Sharma, S. Adhikary, T. J. Rotter, S. J. Lee, Y. H. Kim, and S. Krishna, *Appl. Phys. Lett.* **99**, 191110 (2011).
- ¹⁵I. L. Kresnikov, N. N. Ledentsov, A. Hoffmann, and D. Bimberg, *Phys. Stat. Sol. (a)* **183**, 207 (2001).
- ¹⁶D. Z.-Y. Ting, S. V. Bandara, S. D. Gunapala, J. M. Mumolo, S. A. Keo, C. J. Hill, J. K. Liu, E. R. Blazejewski, B. Rafol, and Y.-C. Chang, *Appl. Phys. Lett.* **94**, 111107 (2009).
- ¹⁷Z. C. Xu, D. Birkedal, J. M. Hvam, Z. Y. Zhao, Y. M. Liu, K. T. Yang, A. Kanjilal, and J. Sadowski, *Appl. Phys. Lett.* **82**, 3859 (2003).
- ¹⁸F. Hopfer, A. Mutig, M. Kuntz, G. Fiol, D. Bimberg, N. N. Ledentsov, V. A. Shchukin, S. S. Mikhrin, D. L. Livshits, I. L. Krestnikov, and A. R. Kovsh, *Appl. Phys. Lett.* **89**, 141106 (2006).
- ¹⁹F.-I. Lai, H. P. D. Yang, G. Lin, I.-C. Hsu, J.-N. Liu, N. A. Maleev, S. A. Blokhin, and H. C. Kuo, *IEEE J. Sel. Top. Quantum Electron.* **13**, 1318 (2007).
- ²⁰A. Lenz, H. Eisele, J.s Becker, L. Ivanova, E. Lenz, F. Luckert, K. Potschke, A. Strittmatter, U. W. Pohl, D. Bimberg, and M. Dahne, *Appl. Phys. Express* **3**, 105602 (2010).